Storage-ring FEL amplifiers and electron beam longitudinal mode-damping times

G. Dattoli, L. Mezi, P. L. Ottaviani,* A. Renieri, and M. Vaccari*
ENEA, Dipartimento Innovazione, Divisione Fisica Applicata, Centro Ricerche Frascati, C.P. 65, 00044 Frascati, Rome, Italy
(Received 5 September 1997)

We exploit the Fokker-Planck equation to investigate the longitudinal phase-space dynamics of a FEL amplifier operating with a storage ring. We study both standard and optical-klystron configurations and prove that in both cases the damping times of the electron longitudinal modes are modified by the system operating conditions. In particular, they decrease with increasing laser power when the input laser is tuned at the resonant frequency. [S1063-651X(98)00306-7]

PACS number(s): 41.60.Cr

I. INTRODUCTION

Different models have been developed to analyze the evolution of the storage-ring (SR) free-electron laser (FEL) dynamics [1]. Among these, a fairly efficient tool is provided by the Fokker-Planck equation (FPE) [2], which has recently been employed to study the dynamical behavior of the electron-beam longitudinal distribution for a SR FEL amplifier [3]. This preliminary investigation has provided an indication that the damping times of the longitudinal modes depend on the system parameters. They have been shown to be a function of the laser intensity and of the detuning parameter. In this paper we analyze this problem more deeply and show that the damping times of higher-order longitudinal modes is significantly reduced for SR FEL amplifiers operating in either the undulator or optical-klystron (OK) configuration.

The increase of the damping times ensures a more efficient ''cooling'' mechanism and therefore this result appears particularly interesting since, as it will be discussed in the following, it seems to confirm the general tendency, suggested by experimental and numerical studies, that the onset of the FEL interaction acts as a feedback stabilizing mechanism for some kinds of longitudinal instabilities.

The plan of the paper is the following. In Sec. II we study the FPE governing the evolution of the longitudinal phase-space dynamics of a SR electron beam undergoing a FEL amplification in the undulator configuration. We perform a mode expansion based on Hermite functions and prove, by numerical analysis, that the mode damping times are sensitive to the various parameters of the system. In Sec. III we address the same problem for the OK configuration and show that in this case too the mode damping times are affected by the main parameter of the system. Section IV is devoted to concluding remarks. We comment on the link between the present results and other observations related to the inhibition caused by the FEL interaction of microwave instability and potential well distortion effects. Appendixes A and B are devoted to the details of the calculations.

*Present address: ENEA, Dipartimento Innovazione, Centro Ricerche Bologna, Bologna, Italy.

II. SR FEL AMPLIFIERS AND LONGITUDINAL MODE DYNAMICS

The evolution of the longitudinal distribution $f(z,\varepsilon,t)$ of an electron beam circulating in a SR and undergoing a FEL interaction can be described by the FPE

$$\frac{\partial f}{\partial t}=\omega_s\left(\frac{c\alpha_c}{\omega_s}\,\varepsilon\,\frac{\partial f}{\partial z}-\frac{\omega_s}{c\alpha_c}\,z\,\frac{\partial f}{\partial \varepsilon}\right)+\frac{1}{T}\,\frac{\partial}{\partial \varepsilon}\left[2\,\frac{T}{\tau_s}\,\varepsilon f+\left(\left\langle\frac{\delta\varepsilon^2}{2}\right\rangle+DT\right)\,\frac{\partial f}{\partial \varepsilon}\right], \tag{2.1}$$

where ε is the relative energy, ω_s the synchrotron frequency, α_c the momentum compaction, T the machine revolution period, and D the radiation noise diffusion coefficient. Equation (2.1) reduces to the usual FPE of the SR synchrotron motion when the laser is off ($\langle\delta\varepsilon^2\rangle=0$). In this last case, the stationary solution ($\partial f/\partial t=0$) is provided by

$$f_0(z,\varepsilon)=\frac{1}{2\pi\sigma_z\sigma_\varepsilon}\exp\left[-\frac{1}{2}\left(\frac{z^2}{\sigma_z^2}+\frac{\varepsilon^2}{\sigma_\varepsilon^2}\right)\right], \tag{2.2}$$

where

$$\sigma_\varepsilon=\sqrt{\frac{D\tau_s}{2}},\quad \sigma_z=\frac{c\alpha_c}{\omega_s}\,\sigma_\varepsilon\,. \tag{2.3}$$

By rescaling the variable according to the prescription

$$\theta=\omega_s t,\qquad \overline{\omega_s}=\omega_s\tau_s\,,\qquad x=\frac{z}{\sigma_z},\qquad y=\frac{\varepsilon}{\sigma_\varepsilon} \tag{2.4a}$$

and by recalling that

$$\langle\delta\varepsilon^2\rangle=A\left[\frac{\sin(\nu/2)}{\nu/2}\right]^2,\quad \nu=2\pi N\,\frac{\omega_0-\omega}{\omega_0}, \tag{2.4b}$$

we can recast Eq. (2.1) in the form

$$\frac{\partial}{\partial\theta}g=\left(y\frac{\partial}{\partial x}-x\frac{\partial}{\partial y}\right)g+\frac{2}{\overline{\omega}_s}\frac{\partial}{\partial y}\left[yg+\{[1+W\times G[(y+y_0)\mu_\varepsilon]\}]\frac{\partial}{\partial y}g\right], \tag{2.5a}$$

where $\mu_\varepsilon=4N\sigma_\varepsilon$ is the energy-spread inhomogeneous broadening parameter, y_0 is linked to the detuning as discussed below, and

$$W=\frac{1}{\mu_\varepsilon^2}\frac{I}{I_s}\frac{\tau_s}{T}, \tag{2.5b}$$

with I being the laser power density and I_s the FEL power saturation density. Equation (2.5) can be conveniently expanded in terms of harmonic-oscillator functions (see Appendix A)

$$g(x,y,\theta)=\frac{1}{2\pi}\sum_{r,m=0}^{\infty}h_{r+m,m}(\theta)\mathrm{He}_r(x)\mathrm{He}_m(y)\times\exp\left(-\frac{x^2+y^2}{2}\right) \tag{2.6}$$

to get (see also Ref. [3])

$$\frac{d}{d\theta}h_{n,m}=(m+1)h_{m,m+1}-(n-m+1)h_{n,m-1}-\frac{2m}{\overline{\omega}_s}h_{n,m}+\frac{2W}{\overline{\omega}_s}\sum_{r=0}^{\infty}G_m^r(\mu_\varepsilon,y_0)h_{n-m+r,r}$$

$$(n=0,1,2;\ \ m=0,1,\ldots,n;\ \ h_{n,m}=0\ \text{ for }\ m>n\ \text{ or }\ m,n<0), \tag{2.7}$$

where

$$G_m^r(\mu_\varepsilon,y_0)=\frac{1}{(m-1)!}\frac{1}{\sqrt{2\pi}}\times\int_{-\infty}^{+\infty}\left(\sin c\left[\frac{\pi}{2}(y+y_0)\mu_\varepsilon\right]\right)^2\times\exp\left(-\frac{y^2}{2}\right)\mathrm{He}_{r+1}(y)\mathrm{He}_{m-1}(y)dy. \tag{2.8}$$

It is evident that when the FEL is switched off ($W=0$), coupling occurs only between modes having the same index n, which specifies the order of the mode ($n=1$ dipole, $n=2$ quadrupole, $n=3$ sextupole, etc.). The evolution of the mode can be easily obtained and is characterized by the eigenvalues

$$\lambda_{n,s}^{\pm}=-\frac{n}{\overline{\omega}_s}\pm is\sqrt{1-\frac{1}{\overline{\omega}_s^2}},\quad s\ll m,$$
$$s=0,2,\ldots,n\ \ (\text{even}),\quad s=1,3,\ldots,n\ \ (\text{odd}) \tag{2.9}$$

TABLE I. Even and odd eigenvalues and relevant notations. $\mathcal{N}$ is the number of eigenvalues, $\mathcal{N}_R$ the number of real eigenvalues, $\mathcal{N}_L$ the number of couples of complex conjugate eigenvalues, λ the real eigenvalue, and Re λ the real part of the complex conjugate eigenvalue.

n	$\mathcal{N}$	$\mathcal{N}_R$	$\mathcal{N}_L$	λ	Re λ
1	2	0	1	0	α
2	3	1	1	a	b
3	4	0	2	0	(β,δ)
4	5	1	2	c	(d,e)

(see Appendix A for further comments). It is also evident that the longitudinal mode evolution is characterized by a damping time τ_s/n and by an oscillatory frequency. When $W\neq0$ the problem is no longer amenable for an analytical treatment, modes are coupled, and the damping times become functions of the characteristic quantities of the system, such as, the detuning, the laser intensity, and the inhomogeneous broadening parameter.

Before proceeding further we must stress that the variable y is linked to the FEL detuning parameter by

$$y=\frac{\nu}{\pi\mu_\varepsilon},\qquad \nu=2\pi N\frac{\omega_0-\omega}{\omega_0}, \tag{2.10}$$

where ω_0 is the resonant frequency. Since W is inversely proportional to μ_ε, we introduce for later convenience, namely, to study separately the effect of the energy spread and of the input laser power density, the quantity

$$W=W_0\left[\frac{\mu_\varepsilon^0}{\mu_\varepsilon}\right]^2, \tag{2.11}$$

where μ_ε^0 is the inhomogeneous broadening parameter associated with a reference energy spread and W_0 is the dimensionless input laser power density normalized to μ_ε^0.

The kernel of the problem is contained in the convolution integral (2.8), which fixes the size of the matrices to be involved in the calculation (see Appendix B). The problem is slightly simplified however, by the fact that odd-odd and even-even mode couplings only are allowed at $y_0=0$. The range of values we have considered has allowed us to restrict the size of the matrices to 24×24 for the even modes (up to $n=8$) and to 20×20 for the odd modes (up to $n=7$). In the more general case $y_0\neq0$ even and odd modes are mixed and we have considered 44×44 matrices.

In this way we have obtained reliable eigenvalues for $n=1,3,5$ and $n=2,4,6$. The results of the numerical analysis are shown in Figs. 1–3, which have been divided into two groups of odd ($n=1,3$) and even ($n=2,4$) eigenvalues. We have displayed the dependence vs W_0 in Figs. 1(a) and 1(b), vs ν_0 in Figs. 2(a) and 2(b), and vs μ_ε in Figs. 3(a) and 3(b). The eigenvalues are labeled as indicated in Table I.

In Figs. 1(a) and 1(b) we have reported the real part of the eigenvalues vs W_0. It is evident that the deviation from the

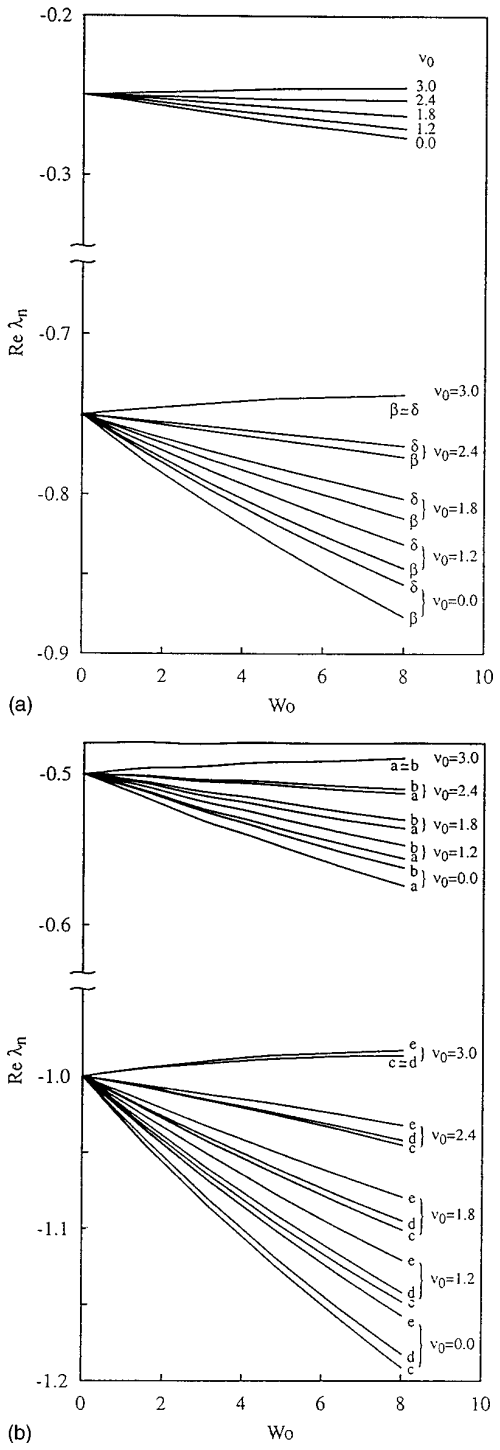

FIG. 1. (a) Real part of the odd eigenvalues vs W_0, for $\overline{\omega_s}=4$ different ν_0 values, $\mu_\varepsilon(0)=0.1$, and $\mu_\varepsilon=0.2$ (undulator configuration). (b) Same as (a) but for the even eigenvalues.

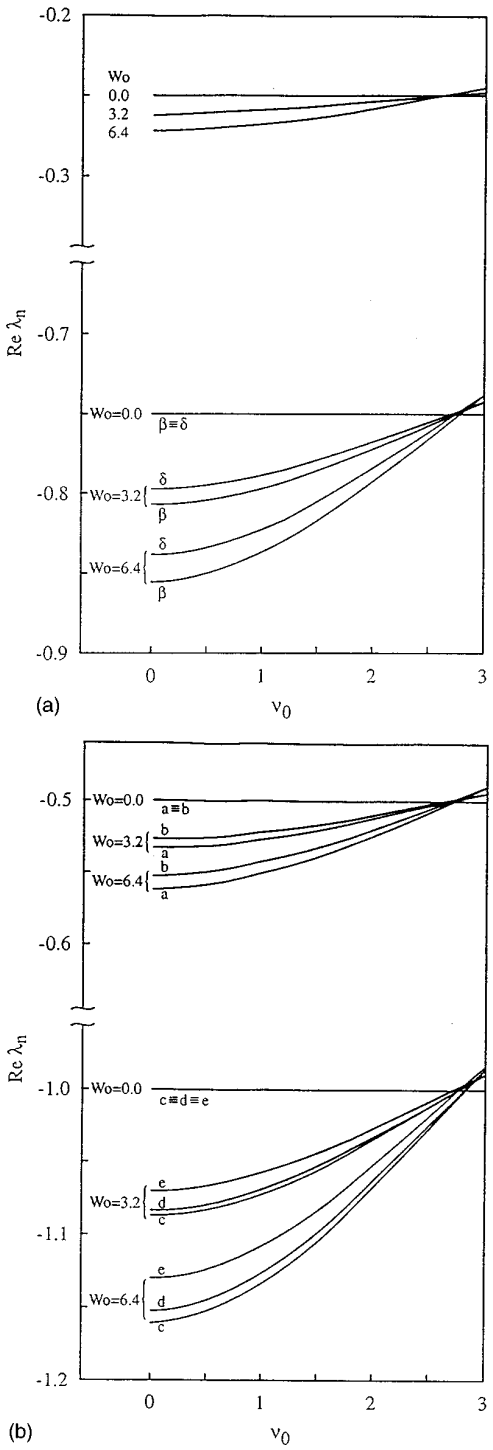

FIG. 2. (a) Real part of the odd eigenvalues vs ν_0 for different W_0 values, with the same parameters as in Fig. 1. (b) Same as (a), but for the even eigenvalues.

natural damping is maximum for $\nu_0\cong 0$ and for larger values of W_0. The effect becomes less significant with increasing ν_0 and for $\nu_0>2.5$ there is the opposite tendency, namely, the eigenvalues decrease (in modulus) and thus the damping times tend to increase. Figures 2(a) and 2(b) describe the behavior of Re λ_n vs μ_ε for fixed W_0. In this case one can see that the effect of damping time reduction is counteracted by larger values of the natural energy spread. This result will be discussed in Sec. IV. Figures 3(a) and 3(b) provide the behavior of the real part of the eigenvalues as a function of the detuning parameter ν_0 (ν_0 is the value of the detuning corresponding to y_0) for different W_0 values. [To give an idea of the number involved in, we note that $W_0=1$ corresponds to a laser input power density of about 10^4 W/cm^2 for $N=50$, $k=3$, $\lambda_u=9$ cm, $\gamma\cong 10^3$, $\tau_s=3\times 10^{-3}$ ms, $T=300$ ns, and $\sigma_{\perp\varepsilon}(0)\sim 10^{-4}$. They confirm, from a different perspective, the results of Fig. 1.

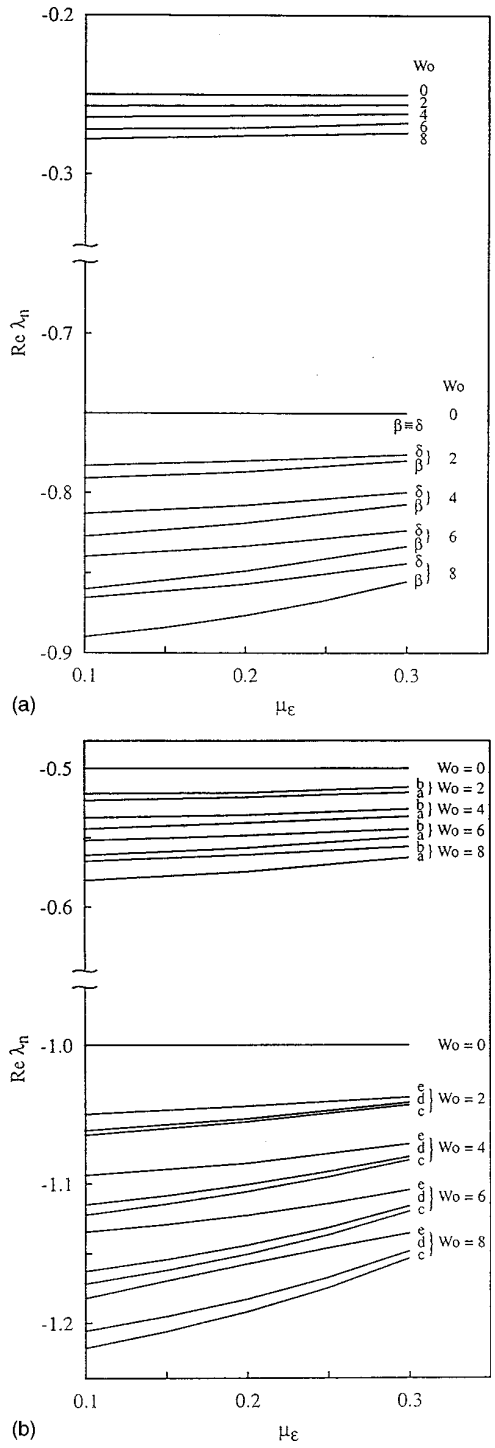

FIG. 3. (a) Real part of the odd eigenvalues vs μ_ε for different W_0 values, $\nu_0 \cong 0$, $\overline{\omega_s}=4$, and $\mu_\varepsilon^0=0.1$. (b) Same as (a), but for the even eigenvalues.

III. STORAGE-RING FEL AMPLIFIERS WITH AN OK CONFIGURATION

The longitudinal dynamics of a SR FEL amplifier, operating with an OK configuration, is governed by the same FPE given in Eqs. (2.1) and (2.7); the only variations are contained in the functions G_m^r, which should take into account the role of the dispersive section and of the consequent optimization to enhance the gain [4]. In particular we get

$$G_m^r(k,y_0)=\frac{1}{2(m-1)!}\frac{1}{\sqrt{2\pi}}\int_{-\infty}^{+\infty} dy\ e^{-y^2/2} \times \mathrm{He}_{r+1}(y)\mathrm{He}_{m-1}(y)\cos\left[\frac{\pi}{2}k(y+y_0)\right], \tag{3.1a}$$

where

$$k=\mu_\varepsilon^{\mathrm{OK}}\sqrt{1+W}, \quad \mu_\varepsilon^{\mathrm{OK}}=8(N+N_d)\sigma_\varepsilon, \tag{3.1b}$$

and N_d is the number of equivalent periods of the dispersive section. The device is composed of two undulators with identical number of periods (N) and length $N\lambda_u$, separated by a dispersive section of length $N_d\lambda_u$.

In Fig. 4 we have reported the real part of the eigenvalues vs W_0 for different ν_0. For small ν_0 values, there is a clear indication that the damping times decrease with increasing W_0. For larger detunings ($\nu_0 \geqslant 2.2$) there is the opposite tendency and the damping times increase. Figure 5 further confirms the results of Eq. (4) and it is evident that Re λ_n is above the natural threshold ($\mathrm{Re}\,\lambda_n|_{W_0=0}=n/\tau_s$) for $\nu_0 \geqslant 2.2$.

IV. CONCLUDING REMARKS

The results described in the previous sections are in fairly good agreement with previous experimental and theoretical works. It has indeed been observed [5] that the onset of the laser is, in many cases, characterized by a partial suppression of the higher-order longitudinal modes. More recent numerical investigations [6] have shown that longitudinal instabilities, like the anomalous bunch lengthening, may be suppressed by the FEL interaction itself. These facts and what has been discussed in the previous sections can be traced back to a common framework. The FEL interaction induces an additional energy spread, which increases with increasing laser intensity. The onset of and the support to the higher-order modes becomes significantly reduced. This effect is more pronounced around small ν_0 values where the induced energy spread is larger. This explains the behavior of Figs. 1 and 2, which show that the suppression effect of the higher-order modes is less efficient with an increasing detuning parameter. The same holds for Fig. 2; in fact, for equivalent values of ν_0 and W_0, the induced energy spread is reduced by increasing values of the inhomogeneous broadening parameter μ_ε.

We must underline that the results of this paper hold for the natural energy spread only. The results of Fig. 3 cannot be extended to the case of an energy spread different from the natural one. We must also underline the peculiar nature of the induced energy spread that is energy dependent and stress that for $\nu_0 > 2.5$, i.e., when the slope of the FEL gain curve becomes negative, the damping times increase. The results of Figs. 4 and 5 relevant to the klystron configuration confirm the above-given interpretation. We note in fact that the cooling effect is larger when the induced energy spread is larger (i.e., for smaller ν_0 and larger W_0).

We may therefore conclude that various indications are converging and seem to confirm that the FEL interaction, with the consequent induction of an energy-dependent energy spread, creates new conditions, which favor the lowest-

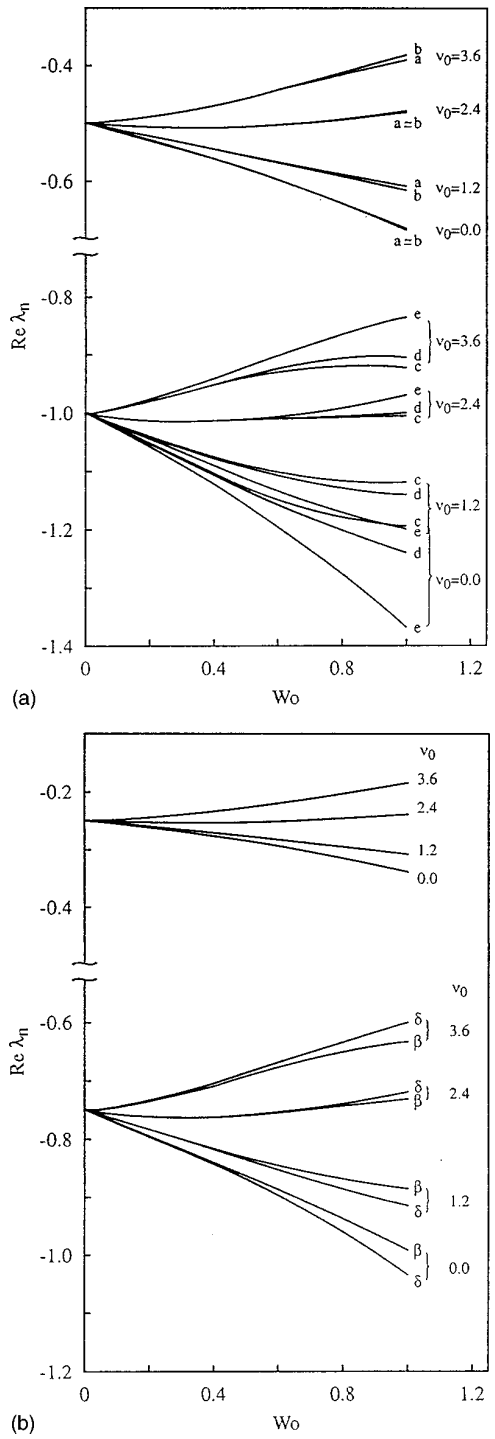

FIG. 4. (a) Real part of the odd eigenvalues vs W_0 for different ν_0 values, $\overline{\omega_s}=4$, and $\tilde{\mu}_e^{\mathrm{OK}}=0.5$ (OK configuration). (b) Same as (a), but for the even eigenvalues.

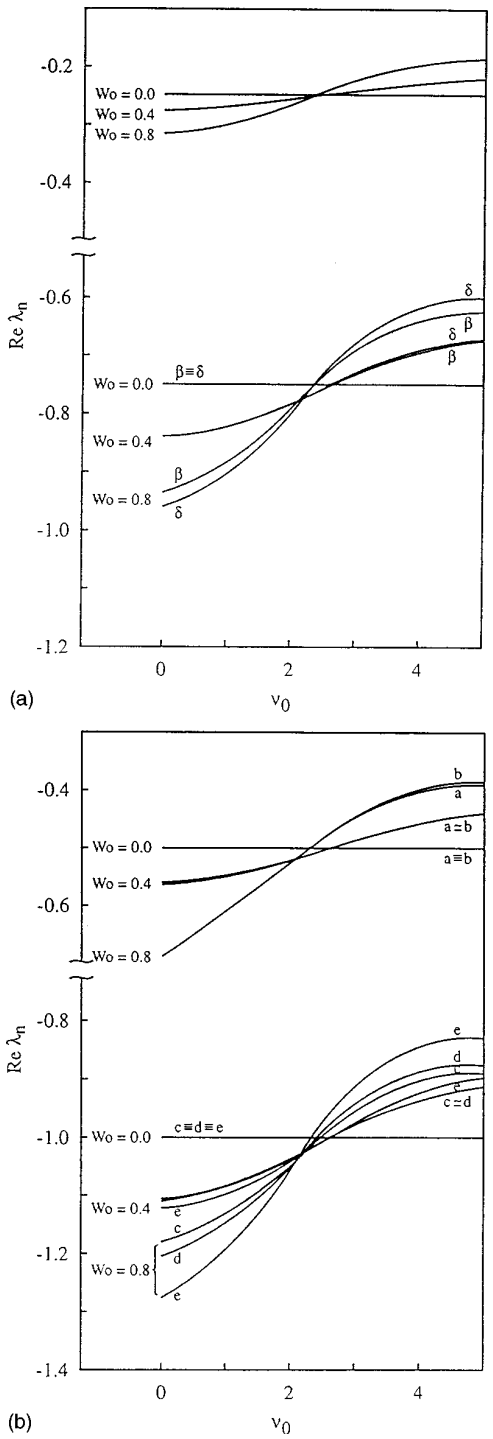

FIG. 5. (a) Real part of the odd eigenvalues vs ν_0 for different W_0 values and the same parameters as in Fig. 4 (OK configuration). (b) Same as (a), but for the even eigenvalues.

order longitudinal modes and provide a suppression mechanism for the longitudinal instabilities.

We must stress, however, that the present treatment is limited to the one-dimensional case. Three-dimensional contributions may modify some aspects of the interaction between electrons and laser light [7,8] and therefore they should be carefully considered within the present context.

As a final remark we underline that our treatment has been limited to the amplifier case, while the experimental results we have referred to are relevant to the oscillator configuration. A more appropriate analysis would require the self-consistent treatment of the evolution of the electron beam and optical field. A simple analysis based on a heuristic one-dimensional oscillator model has provided a preliminary confirmation of the results of this paper.

ACKNOWLEDGMENTS

The authors express their gratitude to Dr. L. Palumbo, Dr. V. Litvinenko, and Dr. M. Migliorati for enlightening discus-

sions on the interplay between FEL and electron-beam dynamics in storage rings. This work was partially supported by CEE Human-Capital and mobility Network No. CHRX-CT 94-0683.

APPENDIX A

To deal with equations of the type (2.7) it is convenient to introduce a column vector $\underline{h}$ that is specified by an index $i \equiv (n,m)$ with $0 \leqslant n \leqslant n_{\max}$, $0 \leqslant m \leqslant n$, so that

$$h_i' = \sum_j A_{i,j} h_j + g_i, \quad j \equiv (s,r), \tag{A1}$$

where

$$A_{i,j} = (m+1)\,\delta_{(s,r),(n,m+1)} - (n-m+1)\,\delta_{(s,r),(n,m-1)} - \frac{2m}{\overline{\omega}_s}\,\delta_{(s,r),(n,m)} + \frac{2W}{\overline{\omega}_s}\,G_r^m\,\delta_{(s,r),(n-m+r,r)}, \tag{A2}$$

where δ denotes the Kronecker delta function and $\underline{g}$ is column vector that is nonzero for n even. In particular we have for $y_0 = 0$ (with $n = 1,3$ and $h' = \hat{A}h$)

$$\hat{A} = \begin{pmatrix} 0 & 1 & 0 & 0 & 0 & 0 \\ -1 & -\frac{2}{\overline{\omega}_s}(1 - WG_1^1) & 0 & 0 & 0 & \frac{2W}{\overline{\omega}_s} G_1^3 \\ 0 & 0 & 0 & 1 & 0 & 0 \\ 0 & 0 & -3 & -\frac{2}{\overline{\omega}_s}(1 - WG_1^1) & 2 & 0 \\ 2\frac{W}{\overline{\omega}_s} G_2^0 & 0 & 0 & -2 & -\frac{4}{\overline{\omega}_s}\left(1 - \frac{W}{2} G_2^2\right) & 3 \\ 0 & \frac{2W}{\overline{\omega}_s} G_3^1 & 0 & 0 & -1 & -\frac{6}{\overline{\omega}_s}\left(1 - \frac{W}{3} G_3^3\right) \end{pmatrix} \tag{A3a}$$

and (with $n = 2,4$ and $\underline{h}' = \hat{A}\underline{h} + \underline{g}$)

$$\hat{A} = \begin{pmatrix} 0 & 1 & 0 & 0 & 0 & 0 & 0 & 0 \\ -2 & -\frac{2}{\overline{\omega}_s}(1 - WG_1^1) & 2 & 0 & 0 & 0 & \frac{2W}{\overline{\omega}_s} G_1^3 & 0 \\ 0 & -1 & -\frac{4}{\overline{\omega}_s}\left(1 - \frac{W}{2} G_2^2\right) & 0 & 0 & 0 & 0 & \frac{2W}{\overline{\omega}_s} G_2^4 \\ 0 & 0 & 0 & 0 & 1 & 0 & 0 & 0 \\ 0 & 0 & 0 & -4 & -\frac{2}{\overline{\omega}_s}(1 - WG_1^1) & 2 & 0 & 0 \\ \frac{2W}{\overline{\omega}_s} G_2^0 & 0 & 0 & 0 & -3 & -\frac{4}{\overline{\omega}_s}\left(1 - \frac{W}{2} G_2^2\right) & 3 & 0 \\ 0 & \frac{2W}{\overline{\omega}_s} G_3^1 & 0 & 0 & 0 & -2 & -\frac{6}{\overline{\omega}_s}\left(1 - \frac{W}{3} G_3^3\right) & 4 \\ 0 & 0 & \frac{2W}{\overline{\omega}_s} G_4^2 & 0 & 0 & 0 & -1 & -\frac{8}{\overline{\omega}_s}\left(1 - \frac{W}{4} G_4^4\right) \end{pmatrix},$$

$$\underline{g} = \begin{pmatrix} 0 \\ 0 \\ \frac{2WG_2^0}{\overline{\omega}_s} \\ 0 \\ 0 \\ 0 \\ 0 \\ \frac{2WG_4^0}{\overline{\omega}_s} \end{pmatrix}. \tag{A3b}$$

APPENDIX B

The integrals appearing in Eqs. (2.8) and (3.1a) involve products of Gaussian functions and Hermite polynomials. They can be expressed in analytical forms, which are reported here for the sake of completeness and to provide further insight into the structure of the problem. We underline that the previous analysis is entirely numerical and the results of this appendix have been used as benchmarks.

We consider therefore the integral

$$I_{m,n}(k,\alpha)=\int_{-\infty}^{+\infty}\cos(ky)e^{-y^2/\alpha}\mathrm{He}_n(y)\mathrm{He}_n(y)dy, \tag{B1}$$

where

$$\mathrm{He}_m(x)=m!\sum_{r=0}^{[m/2]}\frac{(-1)^r x^{m-2r}}{2^r r!(m-2r)!}. \tag{B2}$$

The integral (B1) can be cast in the form

$$I_{m,n}(k,\alpha)=\sqrt{\pi\alpha}e^{-\alpha k^2/4}\,\mathrm{Re}\left[H^{(2)}_{m,n}\left(ik\frac{\alpha}{2},\frac{\alpha}{4}-\frac{1}{2},ik\frac{\alpha}{2},\frac{\alpha}{4}-\frac{1}{2},\frac{\alpha}{2}\right)\right] \tag{B3}$$

if m and n have the same parity; otherwise it vanishes identically. $H^{(2)}_{m,n}$ are two index Hermite polynomials specified as [8]

$$H^{(2)}_{m,n}(x,z,y,w,k)=\sum_{q=0}^{\min(m,n)}(-1)^q q!k^q\binom{m}{q}\times\binom{n}{q}H_{m-q}(x,z)H_{n-q}(y,w), \tag{B4}$$

where $H_m(x,y)$ are Kampé–de Feriet polynomials specified by [8]

$$H_m(x,y)=m!\sum_{r=0}^{[n/2]}\frac{y^r x^{m-2r}}{r!(m-2r)!}. \tag{B5}$$

By using the identity

$$\mathrm{Re}\left[H^{(2)}_{m,n}\left(ik\frac{\alpha}{2},\frac{\alpha}{4}-\frac{1}{2},ik\frac{\alpha}{2},\frac{\alpha}{4}-\frac{1}{2},-\frac{\alpha}{2}\right)\right]=(-1)^{(m+n)/2}\sum_{r=0}^{\min(m,n)}(-1)^r r!\binom{m}{r}\binom{n}{r}\times H_{m+n-2r}\left(\alpha\frac{k}{2},\frac{1}{2}-\frac{\alpha}{4}\right), \tag{B6}$$

we obtain the result

$$I_{m,n}(0,\alpha)=\sqrt{\pi\alpha}(-1)^{(m+n)/2}\sum_{r=0}^{\min(m,n)}(-1)^r r!\binom{m}{r}\times\binom{n}{r}\frac{(m+n-2r)!}{\left[\frac{m+n}{2}-r\right]!}\left(\frac{1}{2}-\frac{\alpha}{4}\right)^{(m+n)/2-r}, \tag{B7}$$

which can be exploited to get an analytical expression for G^r_m.

By noting indeed that the approximation

$$\left(\frac{\sin x/2}{x/2}\right)^2\cong\exp\left(-\frac{x^2}{11}\right) \tag{B8}$$

holds (see Fig. 6) by keeping $y_0=0$, and by defining

$$\alpha(\mu_\varepsilon)=\left[\frac{(\mu_\varepsilon\pi)^2}{11}+\frac{1}{2}\right]^{-1}, \tag{B9}$$

we end up with

$$G^n_m(\mu_\varepsilon,0)\cong\frac{\sqrt{\alpha(\mu_\varepsilon)}}{(m-1)!}\frac{(-1)^{(m+h)/2}}{\sqrt{2}}\sum_{r=0}^{\min(m-1,n+1)}(-1)^r r!\times\binom{m-1}{r}\binom{n+1}{r}\frac{(m+n-2r)!}{\left[\frac{m+n}{2}-r\right]!}\times\left[\frac{1}{2}-\frac{1}{4}\alpha(\mu_\varepsilon)\right]^{(m+n)/2-r}. \tag{B10}$$

An idea of the validity of the approximation (A10) is offered by Fig. 7.

The G^n_m relevant to the OK configuration can be evaluated without any approximation. We note indeed that by setting $\alpha=2$ in Eq. (A3) we find

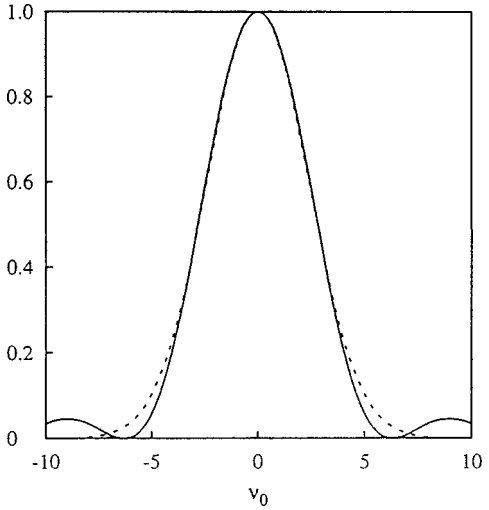

FIG. 6. Comparison between $[\sin c(\nu/2)]^2$ (continuous line) and the approximant Gaussian $\exp(-\nu^2/11)$.

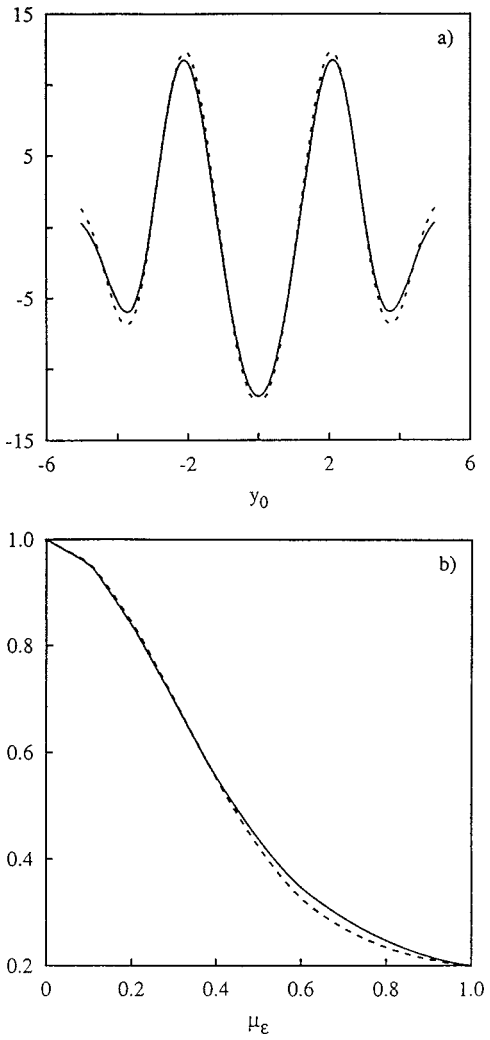

FIG. 7. (a) $G_3^7(\mu_\varepsilon, y_0)$ ($\mu_\varepsilon = 1$) vs exact integration (dotted line) and approximate integration (continuous line). (b) $G_3^1(0, \mu_\varepsilon)$ vs μ_ε exact integration (continuous line) and approximate integration (dotted line).

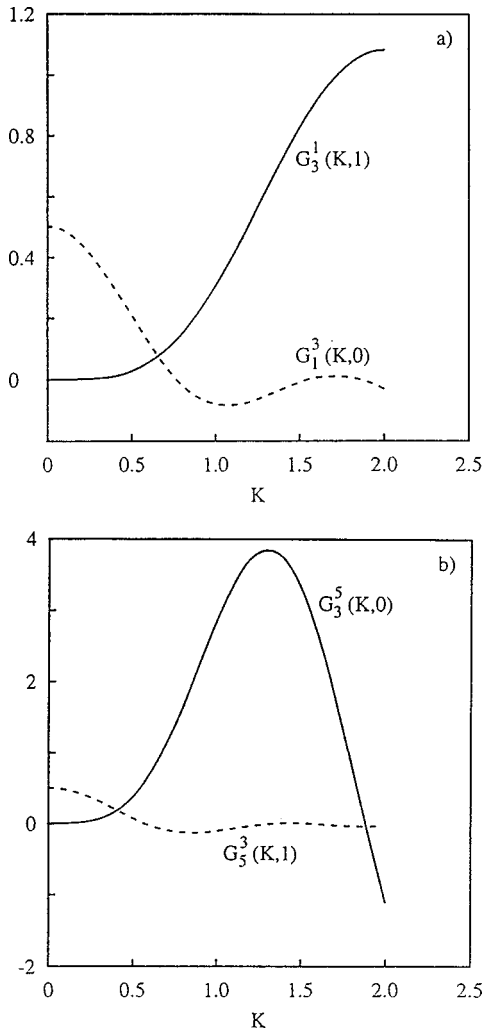

FIG. 8. $G_m^r(k, y_0)$ vs k for different values of y_0.

$$I_{m,n}(k, \tfrac{1}{2}) = \sqrt{2\pi}(-1)^{(m+n)/2}\ \mathrm{Re}[H_{m,n}(ik)]\exp\left(-\frac{k^2}{2}\right), \tag{B11a}$$

where

$$H_{m,n}(x) = m!n!\sum_{q=0}^{\min(m,n)} q!\binom{m}{q}\binom{n}{q}x^{m+n-2q}, \tag{B11b}$$

thus finally getting

$$G_m^n(k, y_0) = \frac{1}{2(m-1)!}\ \mathrm{Re}[H_{m-1,n+1}(ik)e^{iky_0}]\exp\left(-\frac{k^2}{2}\right). \tag{B12}$$

The behavior of $G_m^n(k, y_0)$ for different k and y_0 values is shown in Fig. 8.

[1] See, e.g., D. A. G. Deacon and J. M. Ortega, in *Laser-Handbook*, edited by W. B. Colson, C. Pellegrini, and A. Renieri (North-Holland, Amsterdam, 1990), Vol. VI, p. 345.

[2] For an introduction to the Fokker-Planck equation see, e.g., J. Prigogine, *Non-Equilibrium Statistical Mechanics* (Interscience, New York, 1962), p. 64.

[3] G. Dattoli, L. Giannessi, and A. Renieri, Opt. Commun. **123**, 353 (1996); N. A. Vinokurov and A. S. Skrinsky (unpublished).

[4] W. B. Colson, in *Laser-Handbook* (Ref. [1]), p. 161.

[5] M. Billardon *et al.*, Phys. Rev. Lett. **51**, 1652 (1983); M. Couprie *et al.*, Phys. Rev. A **44**, 1301 (1991); in Proceedings of the *Third Particle Accelerator Conference, Berlin, 1992*, edited by H. Henke, H. Homeyer, and Ch. Petit-Jean-Genaz (Editions

Frontiers, Berlin, 1992), p. 623.
[6] G. Dattoli, A. Renieri, and G. K. Voykov, Phys. Rev. E **55**, 2056 (1997).
[7] V. N. Litivinenko, Nucl. Instrum. Methods Phys. Res. A **359**, 50 (1995).
[8] G. Dattoli and A. Torre, *Theory and Applications of Generalized Bessel Functions* (Aracne, Rome, 1996), and references therein.